ELSEVIER

Materials Science and Engineering B66 (1999) 46–49

MATERIALS SCIENCE & ENGINEERING B

www.elsevier.com/locate/mseb

Study of dopant-dependent band gap narrowing in compound semiconductor devices

V. Palankovski *, G. Kaiblinger-Grujin, S. Selberherr

Institute for Microelectronics, TU Vienna, Gusshausstrasse 27–29, A-1040, Vienna, Austria

Abstract

Band gap narrowing (BGN) is one of the crucial heavy-doping effects to be considered for bipolar devices. Using a physically-based approach (E.F. Schubert, Doping in III-V Semiconductors, Cambridge University Press, 1993), we suggest a new BGN model which considers the semiconductor material and the dopant species for arbitrary finite temperatures. This unified treatment is especially useful for accurate device simulation. A comparison with experimental data and other existing models is presented and study of BGN in III-V group semiconductors is performed. Finally, as a particular example we investigated with our two-dimensional device simulator MINIMOS-NT (Simlinger et al., Simulation of submicron double-heterojunction high electron mobility transistors with MINIMOS-NT, IEEE Trans. Electron. Devices, Vol. 44, 1997, pp. 700–707), the electrical behavior of a graded composition Si/SiGe HBT using a hydrodynamic transport model.

Keywords: Band gap narrowing; Compound semiconductors; Device physics; HBTs; Modeling; Simulation

1. Introduction

Many papers were dedicated to band gap narrowing in semiconductors in the last 20 years (e.g. [2,3]). Despite all of this, the optimal ratio between accuracy of the results on the one hand, and the simplicity of model implementation on the other, appears still not to be achieved. Commercial device simulators, such as ATLAS [4], DESSIS [5], and MEDICI [6], use the logarithmic fit models for band gap narrowing in Si, which are simple to implement, but deliver unphysical values for definite doping levels. The models proposed by del Alamo et al. [7], and Bennet and Wilson [8] cannot be used for concentrations below 10^{18} cm^{-3}, because an unrealistic increase of BGN is obtained. The established model after Slotboom et al. [2], and the model after Klaasen et al. [3], deliver too low values for concentrations of 10^{19} cm^{-3} and above. The functional form of models for Si is used for models for other materials (e.g. III-V compounds) or the BGN effect is left completely ignored. Comparison of these models with the model from this work, and with experimental data for Si is shown in Fig. 1. The physical limit our model offers (0 meV in the case of undoped materials), the physically sound explanation of some existing effects it gives, the ability to treat various semiconductor materials and dopants and the simplicity of the model make it very applicable for device simulation purposes.

2. Physical background of the new model

The basic assumption in our model is that BGN is a result of five types of many-body interactions (electron-electron, electron-impurity, hole-hole, hole-impurity, and electron-hole). At high doping concentrations we assume that electron-impurity contribution is dominant. Although BGN is very difficult to model rigorously due to the multiple carrier interactions one can approximate the energy shift to first order by the classical self-energy of the electron in the field of an ionized impurity [1]. Thus we obtain:

$$\Delta E_g = e \cdot \lim_{r \to 0} [V_s(r) - V(r)] \tag{1}$$

$$V(r) = \frac{1}{(2 \cdot \pi)^3} \int V(q)\, e^{i \cdot \mathbf{q} \cdot \mathbf{r}}\, d\mathbf{q} \tag{2}$$

Here $V_s(r)$ and $V(r)$ denote the screened and unscreened Coulomb potentials of the impurity, respectively.

* Corresponding author.

0921-5107/99/$ - see front matter
PII: S0921-5107(99)00118-X

Equation 1 represents the change in the electrostatic energy of the impurity before and after the electron gas redistribution. If the potential of a point-like impurity is assumed, the Fourier transform of the scattering potential is expressed by Equation 3, where Z and N are the atomic number and the number of electrons of a given material, β denotes the inverse Thomas–Fermi length, and $\mathscr{F}_j(x)$ is the Fermi integral of order j [9]. This approach leads to a simple BGN model [1] given by Equation 5:

$$V(q) = \frac{e^2}{\varepsilon_0 \cdot \varepsilon_r} \cdot \left(\frac{Z - N}{q^2 + \beta^2} \right) \tag{3}$$

$$\beta^2 = \frac{n \cdot e^2}{\varepsilon_0 \cdot \varepsilon_r \cdot k_B \cdot T} \cdot \frac{\mathscr{F}_{-1/2}(\eta)}{\mathscr{F}_{1/2}(\eta)} \tag{4}$$

$$\Delta E_g = -\frac{e^2 \cdot \beta}{4 \cdot \pi \, \varepsilon_0 \cdot \varepsilon_r} \tag{5}$$

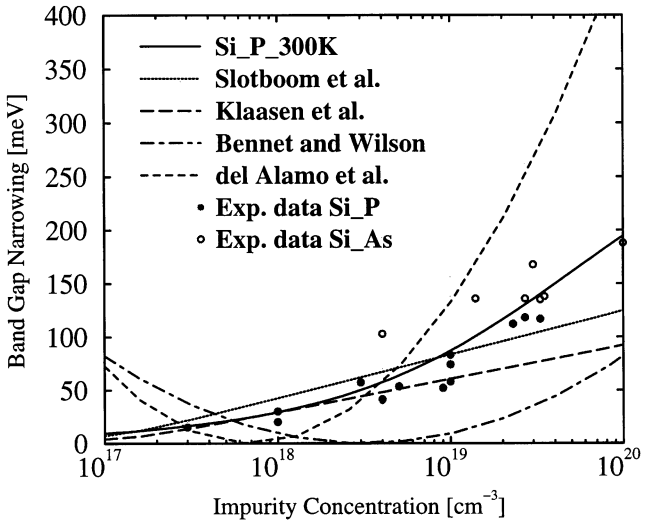

Fig. 1. Comparison with models used in other device simulators.

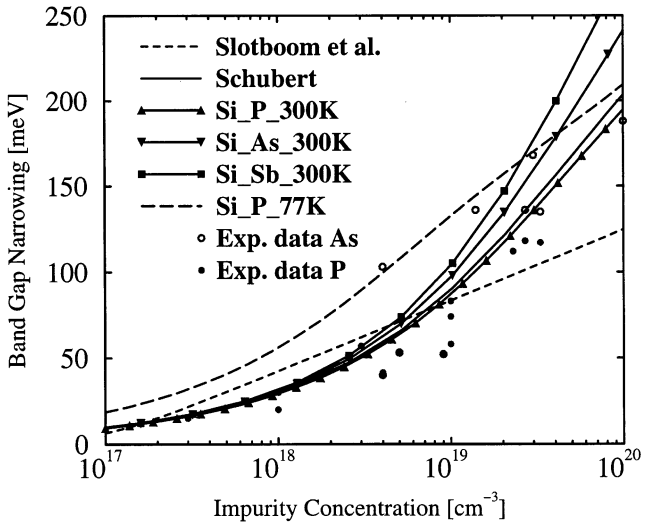

Fig. 2. Influence of the dopant material on BGN in n-Si.

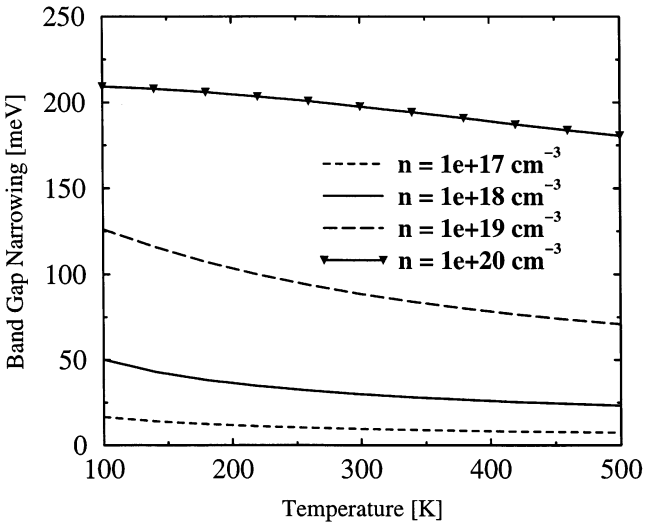

Fig. 3. Temperature dependence of BGN in n-Si.

Removing the point-charge approximation yields a refined model. The charge density of the impurity can be accounted for by an atomic form factor F. Following the work [10] the impurity potential takes the form

$$V(q) = \frac{e^2}{\varepsilon_0 \cdot \varepsilon_r} \cdot \left(\frac{Z - F(q, \alpha)}{q^2 + \beta^2} \right) \tag{6}$$

$$F(q, \alpha) = \frac{N \cdot \alpha^2}{q^2 + \alpha^2} \tag{7}$$

Solving Equation 2 using Equations 6 and 7, and then replacing $V(r)$ in Equation 1, leads to the final expression for the energy shift:

$$\Delta E_g = -\frac{e^2 \cdot \beta}{4 \cdot \pi \cdot \varepsilon_0 \cdot \varepsilon_r} \cdot \left[\frac{\beta \cdot N_I}{\beta + \alpha_I^2} - \frac{\beta \cdot N_{SC}}{\beta + \alpha_{SC}^2} + Z_I - N_I \right]. \tag{8}$$

The subscripts SC and I refer to a semiconductor and impurity, respectively. α can be interpreted as a size parameter of the electron charge density and α_0 is the Bohr radius. They are expressed as:

$$\alpha = \frac{Z^{1/3}}{c_k \cdot \alpha_0 \cdot \varepsilon_r} \cdot \frac{1 - 2 \cdot \left(\frac{Z}{N} \right)}{\frac{5}{3} - 4 \cdot \left(\frac{Z}{N} \right)^{1/3}} \tag{9}$$

$$c_k = \frac{\Gamma(4/3)}{2} \cdot \left(\frac{3 \cdot \pi}{4} \right)^{2/3} \cdot \left(\frac{3}{5} \right)^{7/3} \approx 0{,}24. \tag{10}$$

The size parameter α uses $\varepsilon_r = 1$, which is the most pessimistic estimation, because it is still not clarified which value for ε_r in the range between 1 and ε_{SC} isvalid at microscopic level. Even though the influence of the dopant type is reduced to a minimum this way, our model still delivers different results at 300 K in agreement with experiment [11] (see Fig. 2).

The temperature dependence of the BGN in Si is shown in Fig. 3. Neglecting the stronger BGN at 77 K, especially for doping levels about 10^{19} cm^{-3}, may result in an error of about 50%. Therefore, even larger errors might be introduced into the simulation results, with respect to the electrical device characteristics. In the case of III-V semiconductors our model delivers a comparatively weaker BGN temperature dependence. Similar observations were done in the case of p-GaAs in [12,13]. Thus, our BGN model is the first theoretically derived model predicting different shifts for various dopant species and taking temperature into account.

3. Extending the new model to compounds

Our model extends its validity also for compound semiconductors by material composition dependent relative DOS masses for electrons and holes, on the one hand, and permitivity, on the other hand. The values used for the semiconductor electron number are calculated in a similar way. In Fig. 4 we present the results for boron and gallium doped SiGe for different Ge contents. The decrease of the BGN with increase of the Ge fraction was already experimentally observed in [14,15]. Our theoretical approach explains this effect by the decreased valence band density of states and increase of the relative permitivity in the SiGe alloy.

In the case of p-type GaAs we obtain good agreement with experimental data [12,13]. The few available experimental data for n-type GaAs suggest sometimes lower [16] (open triangles in Fig. 5) values for BGN and more often higher [17] (filled triangles) than our model delivers. This appears to emphasize the importance of modeling BGN in III-V semiconductors, rather than leaving this effect unconsidered, which is the case with the most device simulators.

Experiments showed higher BGN in n-InP than n-GaAs [18]. Higher conduction band density of states and lower relative permitivity explain the expected higher values for BGN in AlAs and GaP (Fig. 6) than in InP, GaAs and InAs. The parameter values are taken from [19].

4. Simulation results

As a particular example the electrical behavior of SiGe HBT was studied at different temperatures using a hydrodynamic transport model. The device structure used is rather conventional and is not discussed in this work. Our investigations were performed in a comparative way for different dopant species and concentrationsusing the new models and the old ones. In Fig. 7 we present the Gummel plots for SiGe HBT at 77 K and 300 K obtained with the model of Slotboom et al. [2] (Model 1) and with our new model (Model 2). Note the signifi-

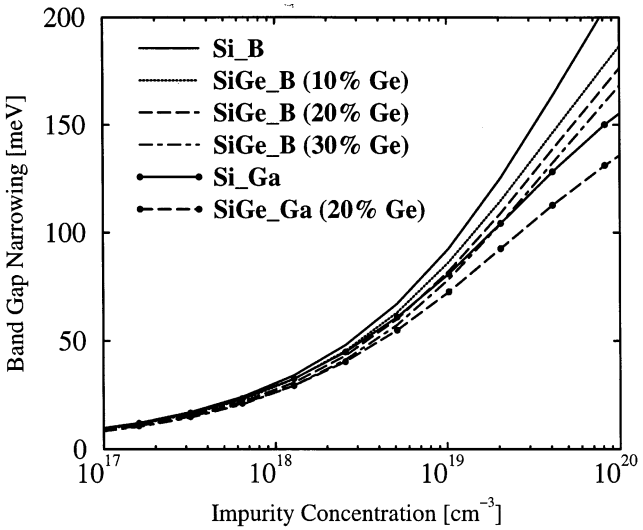

Fig. 4. Influence of the dopant type and Ge content in p-SiGe.

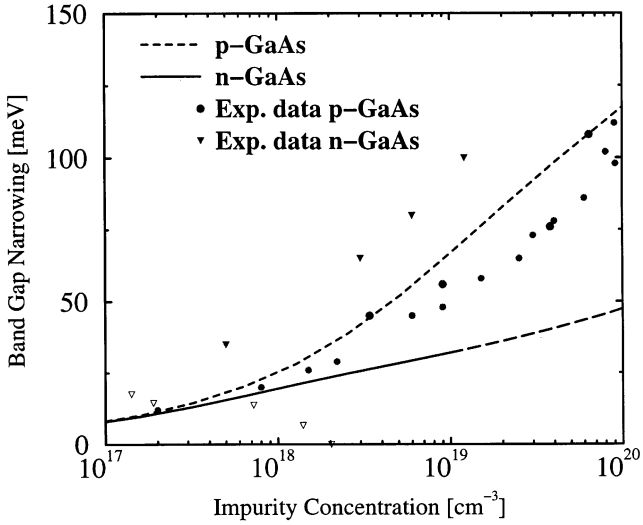

Fig. 5. BGN in GaAs compared with experiment.

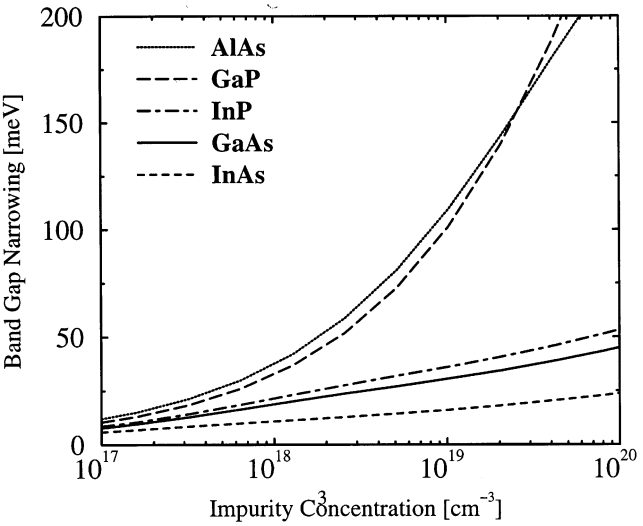

Fig. 6. BGN for different n-type binary compounds.

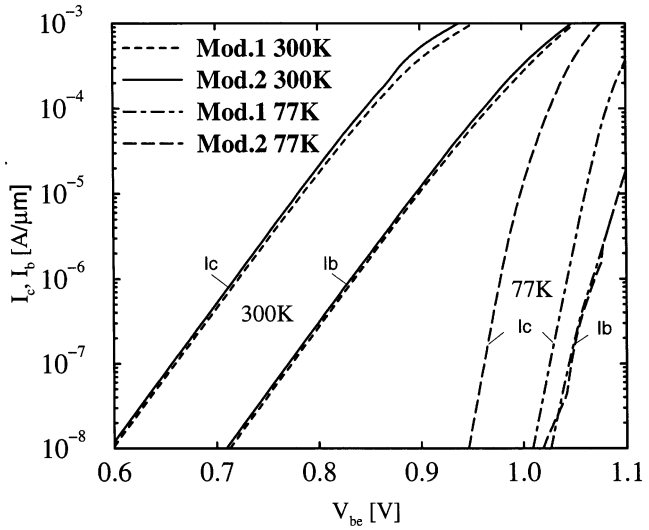

Fig. 7. Gummel plots at $V_{ce} = 2$ V for Models 1 and 2.

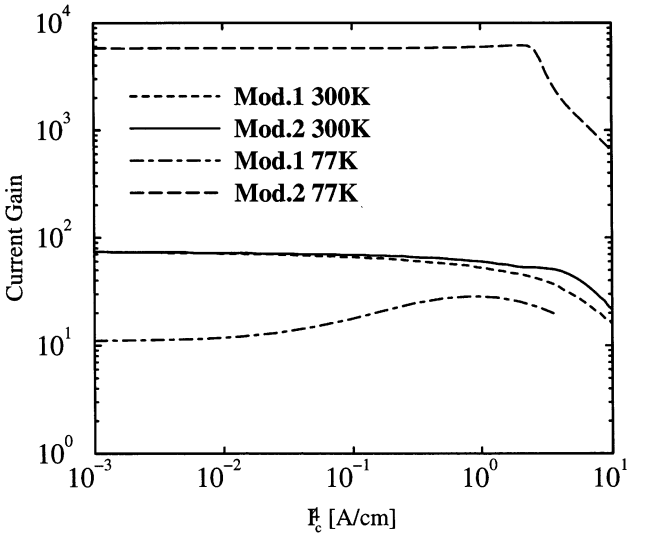

Fig. 8. Current gain versus collector current for Models 1 and 2.

cant difference in the current density values at 77 K, resulting in a higher current gain with the new model (Fig. 8), which is confirmed by experiments.

5. Conclusion

In summary, a new physically based analytical band gap narrowing model is presented. It accounts for different dopants and is extended to compound semiconductors. The agreement with experimental data which, when available, are still rather uncertain is shown. In comparison with other existing models used for device simulation, the superiority of our new model is underlined. Finally, the important impact on the HBT device performance is studied.

Acknowledgements

This work is supported by Siemens AG, Munich, Germany.

References

[1] E.F Schubert, Doping in III-V Semiconductors, Cambridge University Press, Cambridge, 1993.
[2] J.W. Slotboom, H.C. de Graaff, Measurements of bandgap narrowing in Si bipolar transistors, Solid-State Electron. 19 (1976) 857–862.
[3] D.B.M. Klaassen, J.W. Slotboom, H.C. de Graaff, Unified apparent bandgap narrowing in n- and p-type silicon, Solid-State Electron. 35 (2) (1992) 125–129.
[4] ATLAS User's Manual, SILVACO International, 2nd ed, Santa Clara, USA, March 1994.
[5] Integrated Systems Engineering AG, DES515-lSE, ISE TCAD Release 5.0, Part 16, ISE, Zurich, Switzerland, March 1998.
[6] Technology Modeling Associates, TMA Medici, Two-Dimensional Device Simulation Program, Version 4.0 User's Manual, TMA, Sunnyvale, CA October 1997.
[7] J.A. Del Alamo, E. Swirhun, R.M. Swanson, Simultaneous measuring of hole lifetime, hole mobility and bandgap narrowing in heavily doped n-type silicon, Int. Electron. Devices Meet., (1985) 290–293.
[8] H.S. Bennet, C.L. Wilson, Statistical comparisons of data on band-gap narrowing in heavily doped silicon: electrical and optical measurements, J. Appl. Phys. 55 (10) (1984) 3582–3587.
[9] D.K. Ferry, Semiconductors, Macmillan, New York, 1991.
[10] G. Kaiblinger-Grujin, H. Kosina, S. Selberherr, Influence of the doping element on the electron mobility in n-silicon, J. Appl. Phys. 83 (6) (1998) 3096–3101.
[11] J.-S. Park, A. Neugroschel, F.A. Lindholm, Comments on determination of bandgap narrowing from activation plots, IEEE Trans. Electron. Devices 33 (7) (1986) 1077–1078.
[12] Z.H. Lu, M.C. Hanna, A. Majerfeld, Determination of band gap narrowing and hole density for heavily C-doped GaAs by photoluminescence spectroscopy, Appl. Phys. Lett. 64 (1) (1994) 88–90.
[13] B.R Yan, J.S. Luo, Q.L. Zhang, Study of band-gap narrowing effect and nonradiative recombination centers for heavily C-doped GaAs by photoluminescence spectroscopy, J. Appl. Phys. 77 (9) (1995) 4822–4824.
[14] Z. Matutinovic-Krstelj, V. Venkataraman, E.J. Prinz, J.C. Sturm, C.W. Magee, A comprehensive study of lateral and vertical current transport in Si/$Si_{1-x}Ge_x$/Si HBT's, Int. Electron. Devices Meet., (1993) 87–90.
[15] M. Libezny, S.C. Jain, J. Poortmans, M. Caymax, J. Nijs, R. Mertens, K. Werner, R. Balk, Photoluminescence determination of the Fermi energy in heavily doped strained $Si_{1-x}Ge_x$ layers, Appl. Phys. Lett. 64 (15) (1994) 1953–1955.
[16] E.S. Harmon, M.R. Melloch, M.S. Lundstrom, Effective band-gap shrinkage in GaAs, Appl. Phys. Lett. 64 (4) (1994) 502–504.
[17] H. Yao, A. Compaan, Plasmons, photoluminescence and band-gap narrowing in very heavily doped n-GaAs, Appl. Phys. Lett. 57 (2) (1990) 147–149.
[18] R.M. Sieg, S.A. Ringel, Reabsorption, band gap narrowing and the reconciliation of photoluminescence spectra with electrical measurements for epitaxial n-InP, J. Appl. Phys. 80 (1) (1996) 448–458.
[19] A. Katz, Indium Phosphide and Related Materials, Artech House, Boston, MA, 1992.